AIMS Environmental Science, 11(2): 157–183.
DOI: 10.3934/environsci.2024009
Received: 05 January 2024
Revised: 12 March 2024
Accepted: 21 March 2024
Published: 03 April 2024

http://www.aimspress.com/journal/ environmental

Research article

ANN for the prediction of isobutylene dimerization through catalytic distillation for a preliminary energy and environmental evaluation

Daniel Chuquin-Vasco[1,*], Geancarlo Torres-Yanacallo[2], Cristina Calderón-Tapia[3], Juan Chuquin-Vasco[4], Nelson Chuquin-Vasco[4] and Ramiro Cepeda-Godoy[5]

[1] Ingeniería Industrial, Universidad Nacional de Chimborazo, Riobamba
[2] SOLMA, Advanced Mechanical Solutions, Mechanical Engineering, and Construction Services
[3] Escuela Superior Politécnica de Chimborazo (ESPOCH), Environmental Engineering Career
[4] Escuela Superior Politécnica de Chimborazo (ESPOCH), Mechanical Engineering Career
[5] Escuela Superior Politécnica de Chimborazo (ESPOCH), Chemical Engineering Career, Safety, Environment and Engineering Research Group (GISAI)

*** Correspondence:** Email: daniel.chuquin@unach.edu.ec; Tel: +593998163018.

Abstract: This study aimed to develop an artificial neural network (ANN) capable of predicting the molar concentration of diisobutylene (DIB), 3,4,4-trimethyl-1-pentene (DIM), and tert-butyl alcohol (TBA) in the distillate and residue streams within three specific columns: reactive (CDC), high pressure (ADC), and low pressure (TDC). The process simulation was conducted using DWSIM, an open-source platform. Following its validation, a sensitivity analysis was performed to identify the operational variables that influenced the molar fraction of DIB, DIM, and TBA in the outputs of the three columns. The input variables included the molar fraction of isobutylene (IB) and 2-butene (2-Bu) in the butane (C4) feed, the temperature of the C4 and TBA feeds, and the operating pressure of the CDC, ADC, and TDC columns. The network's design, training, validation, and testing were performed in MATLAB using the Neural FittinG app. The network structure was based on the Bayesian regularization (BR) algorithm, that consisted of 7 inputs and seven outputs with 30 neurons in the hidden layer. The designed, trained, and validated ANN demonstrated a high performance, with a mean squared error (MSE) of 0.0008 and a linear regression coefficient (R) of 0.9946. The statistical validation using an analysis of variance (ANOVA) (p-value > 0.05) supported the ANN's capability to reliably predict molar fractions. Future research will focus on the in-situ validation of the predictions and explore hybrid technologies for energy and environmental optimization in the process.

Keywords: ANN; diisobutylene; DWSIM; distillation; tert-butyl alcohol

1. Introduction

Since its discovery in 1857, the widespread use of gasoline, primarily as a source of energy for internal combustion engines, has raised significant environmental concerns. The gases produced during gasoline combustion are known to contribute to the greenhouse effect due to their composition. Additionally, certain additives, such as methyl tert-butyl ether (MTBE), which is used to enhance the octane rating of gasoline, have proven to be equally contaminating, with their current prohibition being considered due to negative impacts on rechargeable water sources [1]. The need for more sustainable alternatives becomes apparent; in this context, isooctane (IO) emerges as a less polluting and versatile option. Beyond its traditional use as a fuel, IO stands out as a raw material in manufacturing essential chemicals, such as octophenol and synthetic rubber [2]. In this context, it is urgent to explore technically viable and economically sustainable methods for IO production to address the environmental challenges associated with the conventional use of gasoline and its additives.

1.1. Isobutene dimerization process

The choice of extractant in the isobutene dimerization process significantly impacts the yield and selectivity of the reaction. The most used extractants include polar solvents such as water, alcohols (methanol, ethanol), and ketones (acetone). Water has proven to be a good extractant to remove the isobutene dimer; however, its use may be limited by the solubility of isobutene in water and the possible formation of unwanted byproducts. Alcohols such as methanol and ethanol are attractive alternatives due to their greater affinity for the dimer; however, care must be taken with possible alkylation reactions that could occur between alcohol and isobutene, while acetone is an extractant due to its good selectivity and extraction capacity. However, due to its flammability, its use involves additional costs and safety considerations. According to Liu et al. [3], obtaining MTBE requires two technical routes. The first route involves the alkylation of isobutane with butene. However, this process requires using an alkylation unit with catalysts such as HF or H_2SO_4, which are highly corrosive and toxic compounds, making it technically unfeasible. The second route entails the dimerization of isobutene, followed by hydrogenation. This latter route has been extensively studied in various scientific publications. A significant advantage of this route is that MTBE plants can be easily and economically adapted for IO production [4]. However, the challenge lies in exclusively obtaining diisobutenes (DIB), as mentioned by Honkela & Krause [1]. In addition to diisobutenes, other oligomers such as triisobutenes and tetraisobutenes are produced, which are not helpful as gasoline additives due to their high molecular weights.

Liu et al. [3] investigated the dimerization process using a butane (C4) mixture of 1-butene and isobutene. To enhance the selectivity of high research octane number (RON) dimers, such as 2,4,4-trimethyl pentene-1 and 2,4,4-trimethyl pentene-2, the temperature in the product stream was varied within a range of 30 to 50 ºC. Ethanol was introduced in a molar ratio of 0.1 to 0.5 ethanol/isobutene (EtOH/IB), and an acid ion exchange resin (DH-2) was employed. The results indicated that adding ethanol inhibits the conversion of 1-butene, enhances the selectivity of dimers, and diminishes the temperature's influence on the reaction.

In contrast, Honkela & Krause [1] investigated the impact of methanol and tert-butyl alcohol (TBA) on the conversion of isobutene, the selectivity of dimers, and the deactivation level of the employed ion exchange resin. The reaction occurred in a 50 cm^3 continuous stirred tank reactor (CSTR) at a pressure of 1.5 MPa, thereby utilizing 1 g of catalyst. Two 2 dm feed tanks at 1.8 MPa were employed, one for the liquid isobutene and the other for the polar component and the distillate. The experiments were conducted at 60, 80, and 100 °C temperatures. Their findings revealed that both polar additives enhanced the selectivity of dimers. Notably, TBA did not form MTBE, unlike methanol, which produced substantial quantities of MTBE. Moreover, an inversely proportional relationship was identified between the isobutene conversion and the dimer selectivity.

Although the use of polar components to improve selectivity turns out to be quite an attractive idea, it does not take into account that the additive has to be separated from the product; in the case of TBA, it forms an azeotrope with DIB, which is very difficult to separate by significantly increasing the costs. Talwalkar et al. [4] proposed an alternative that consisted of using reactive distillation columns (RD) to dimerize IB, taking advantage of the difference in volatilities of the IB and the dimers formed to avoid the simultaneous reactions that give rise to the oligomers from the DIBs.

Kamath et al. [5] conducted a comprehensive analysis of the IB dimerization process through simulation, examining the impact of catalyst loading, the position of the C4 feed, and the feed of the polar component on a 30-stage reactive distillation (RD) system. The results revealed that, beyond a Da (Damkohler number) value of 0.5, there was negligible improvement in the selectivity. The optimal placement for the C4 feed was determined to be in the last reactive stage (Stage 26), as descending through the reactive zone increased the selectivity and the conversion. In contrast, the feed of the polar component exhibited an inversely proportional relationship: the higher the position above the reactive zone, the greater the selectivity achieved, though this also corresponded to an increased catalyst quantity, and vice versa.

Despite the advantages of the DR, the design of the columns and the extraction and regeneration of the catalyst constitute essential challenges at the start-up time. In this sense, Kamath et al. [6] proposed two alternatives focused on the cost analysis when choosing the optimal conversion of IB and the desired selectivity for DIBs. The first alternative involved using 8 CSTR reactors in series at 90 ºC, a pressure greater than 15 atm to work in the liquid phase, and a 10-stage distillation column at 6 atm. This conventional configuration directly introduced the C4 feed to a reactor system and subsequently entered the distillation column with recirculation from the top to the reactor feed. The second configuration directs the C4 feed to the column. It sends the product from the top to the reactor system and the polar component, thus reintroducing the output stream into the RD. The results indicate that the second configuration reduces its selectivity below 60% for high conversions (>90% IB), compared to the conventional process that shows a selectivity more significant than 85%. The conventional system is highly competitive in high conversion situations regarding the annual costs [6].

Talwalkar et al. [4] investigated the RD process without polar components using a 3 m pilot RD column. The column consisted of a 1 m reactive zone packed with KATAPAL-S loaded with the T-36 catalyst, and a 2 m non-reactive zone filled with EVERGREEN HYFLUX and covered with glass wool to minimize heat losses to the surroundings. Three experiments were carried out in a continuous regime, varying the operation of the reboiler and the reaction temperature. The results showed conversions of 49.54%, 55.56%, and 59.69%, with selectivities of 90%, 92%, and 93%, respectively. These findings highlight the influence of operating conditions on the efficiency of the RD process without polar components.

1.2. Simulation of distillation processes for n-hexane and ethyl acetate system

Goortani et al. [7] proposed an innovative strategy to enhance the dimerization process using a reactive column. The employed column was 7 meters in height, with two reaction zones and three separation zones, and utilized a feedstream from the NexOCTANE process. The process simulation was conducted using gPROMS, thus allowing for adjusting reaction rates and interfacial areas. The triphasic mass transfer model employed to represent the distillation column revealed a significant savings of 7–11% in cooling and heating services compared to the conventional NexOCTANE process.

Chalakova et al. [8] developed innovative RD techniques for the IB dimerization process. Two distinct concepts of RD were examined, where IB dimerization and IO hydrogenation were carried out either simultaneously (fully integrated) or sequentially (partially integrated). The process and operating conditions were designed using DIVA and ASPEN PLUS, and an economic and performance comparison was conducted against a conventional process design. The first technique involved using a reactive column and a packed-bed reactor for DIB hydrogenation. The second process intensified the operation by integrating the dimerization zone (upper part) and the hydrogenation zone (lower part) in the same RD setup. For both processes, a high IO selectivity of 93.08% and an IB conversion of 98.34% were achieved in the case of partial integration. In contrast, the IB conversion reached 98.24% for the fully integrated process, and the IO selectivity was 93.36%.

1.3. ANN as a prediction tool in chemical industries

The application of artificial neural networks (ANN) in chemical processes arises in response to the limitations inherent to first principles models (FPM). Due to constant changes in operating conditions and the difficulty in establishing fundamental models, the complexity of understanding reaction kinetics in most industrial processes motivates the use of ANNs. These allow the development of non-linear models of physical phenomena based on historical data from industrial plants. However, the advantage of ANNs is that they do not obey the fundamental laws of conservation of mass, energy, and momentum, nor the laws of thermodynamics. Their accuracy depends on the range of data with which they were trained [7,9–11].

The application of ANNs in the chemical industry has facilitated the development of novel methodologies to address operational and process optimization challenges by predicting outcomes derived from process simulation databases. Various networks with different structures have been employed for machine learning and can be classified into supervised and unsupervised categories [12].

For example, Chouai et al. [13] used ANNs to model and control chemical processes, fit the reaction rate data of complex reactions, and determine the pressure-volume-temperature data in refrigerant fluids. This numerical approach seems to be a convenient tool for modeling, except when we are near the critical point, especially for calculating the heat capacity.

Manssouri et al. [14] used an ANN-extreme learning machine model to predict the temperature at the height of a continuous distillation column, thus demonstrating its accuracy through an accurate forecast with a value of root-mean-square-error (RMSE) = 0.0168 using a database of 1000 samples.

On the other hand, Alhajree et al. [15] modeled and optimized a hydrocracking plant using a multilayer feed-forward ANN with a BACK PROPAGATION (BP) training algorithm, computing on 2/3 of a real plant data bank. They determined that temperature was the most influential input parameter in the process and found optimal values of the operating parameters to maximize the production of diesel, kerosene, heavy naphtha (HN), and light naphtha (LN). These optimal values were as follows:

feed, 113.2 m^3/h; reactor temperature, 413 ºC; and H_2 feed, 111.1 MSCM/h.

This study is motivated by the notable absence of prior research utilizing ANNs for predictive purposes in extractive distillation for separating n-hexane and ethyl acetate. The lack of previous investigations underscores the novelty and importance of applying ANN methodologies to this industrial process. Harnessing the predictive capabilities of neural networks in extractive distillation can enhance the efficiency, optimize the operational parameters, and provide valuable insights into separating n-hexane and ethyl acetate.

This study represents an essential advancement in the field due to the current absence of work on using ANNs applied to IB dimerization. The novelty of this topic lies in its unique focus on using an ANN to predict IB dimerization. Furthermore, its importance goes beyond prediction, as it lays the foundation for future studies that involve hybrid optimization methodologies, thus combining genetic algorithms and neural networks.

2. Materials and methods

2.1. Process description

Figure 1 illustrates the dimerization process of isobutylene by catalytic distillation, adapted from [2]. The process consists of three columns: a catalytic distillation column (CDC), an ADC – TBA recovery column, and a TDC – vacuum distillation column to separate the isomers.

The CDC column receives a feed stream of FCC-C4 and a feed stream of recirculated TBA from the ADC column. In CDC, three reactions are carried out as follows: IB + IB, IB+2-Bu, and IB+DIB for the production of DIB, DIM, and TIB, respectively. The reactive zone begins at stage 9 and concludes at stage 78. The operating conditions allow us to obtain a conversion of 99.08% of the IB and a selectivity of 96.03% in DIB because separating the volatile components from the heavy components prevents the oligomerization of the DIB to produce TIB.

Table 1 summarizes the composition of the feed stream entering the CDC catalytic distillation column. Tables 2–4 detail the catalytic, TBA recovery (ADC) operating conditions and isomer separation (TDC) columns. Unlike the conventional process, the ADC column distillate allows TBA recovery, which is recirculated to the CDC column as an inhibitor of IB polymerization. They increase the selectivity of dimers of high economic interest (DIB-DIM). The TDC column allows for the separation of the dimers due to the vacuum conditions they present, thus obtaining a purity of 99.9%wt DIB in the distillate and 98%wt DIM in the residue.

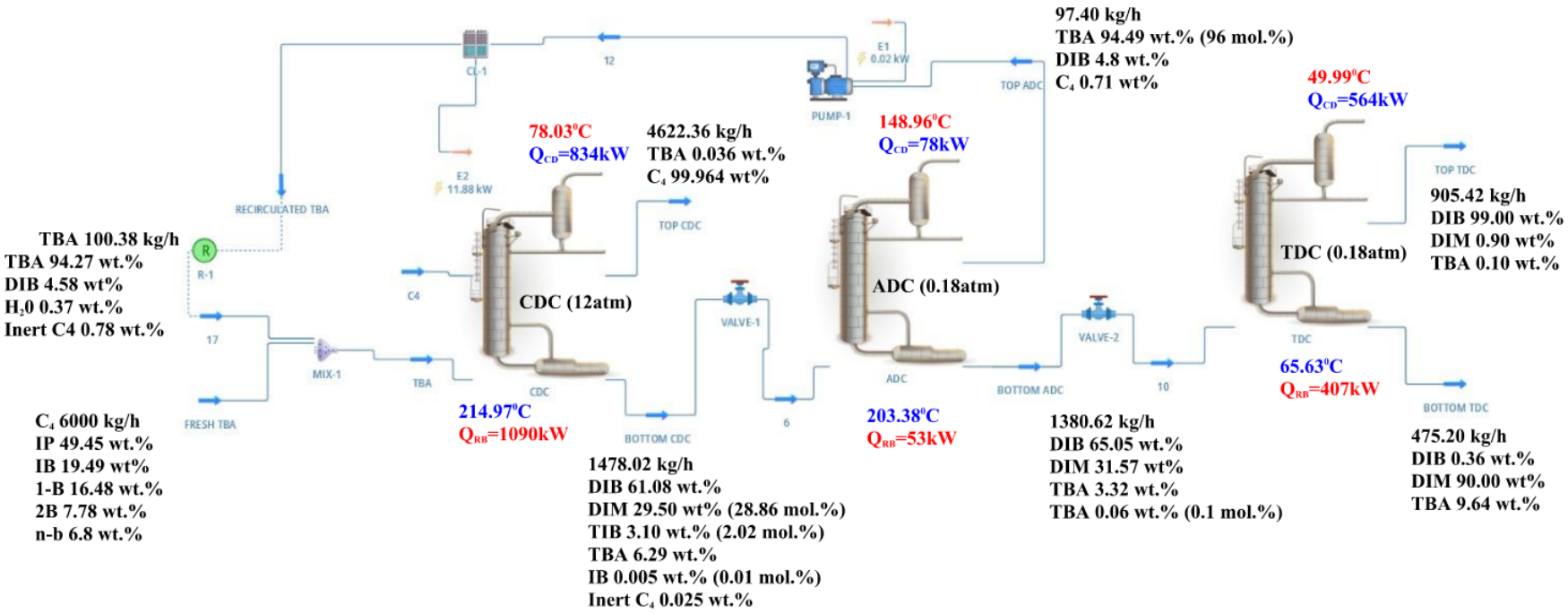

Figure 1. Simulation of the isobutylene dimerization.

Table 1. Feed Conditions to CDC.

Parameter	Quantity	Unit
Pressure	12	atm
Temperature Feed C4 -TBA	25	^{o}C
Feed C4 (mass flow)	6000	kg/h
Initial composition of isobutane	0.4945	-
The initial composition of isobutene	0.1949	-
Initial composition of 1-butene	0.1648	-
Initial composition of 2-butene	0.0778	-
Initial composition of n-butane	0.068	-
Feed TBA (mass flow)	100.38	kg/h
The initial composition of TBA	0.9427	-
Initial composition of diisobutene	0.0.0458	-

Notes: The compositions are given in mass fraction (X); Source: [2]

Table 2. CDC – Catalytic distillation column.

Parameter	Quantity	Unit
Pressure	12	atm
# Column stages*	89	-
# Feed stage TBA*	35	-
# Feed stage C4*	78	-
Reflux ratio (RR)	10	-
Fresh TBA molar flow	1.32	kmol/h
Feed molar flow (C4)	104.85	kmol/h
Condenser duty	834.00	kW
Reboiler duty	1090.00	kW

Notes: *Numbered from the top of the distillation tower; Source: [2]

Table 3. ADC – TBA recovery column.

Parameter	Quantity	Unit
Pressure	8	atm
# Column stages*	88	-
# Feed stage*	69	-
Reflux ratio (RR)	5.35	-
TBA molar flow (recycle stream from ADC)	1.28	kmol/h
Feed molar flow	13.60	kmol/h
Condenser duty	65.24	kW
Reboiler duty	53.00	kW

Notes: * Numbered from the top of the distillation tower; Source: [2]

Table 4. TDC – Vacuum distillation.

Parameter	Quantity	Unit
Pressure	0.18	atm
# Column stages*	122	-
# Feed stage*	61	-
Reflux ratio (RR)	5.71	-
Condenser duty	534.887	MW
Reboiler duty	395.130	MW

Notes: * Numbered from the top of the distillation tower; Source: [2]

The pressure drop was not considered in the simulation of the distillation columns to validate our work with the study carried out by Chen et al. [2], in which the pressure drop in the system was also not considered. Furthermore, the pressure drop is not a parameter that directly affects the catalytic dimerization of IB.

2.2. Methodology

Figure 2 presents the methodological scheme adopted for the development of the ANN. In the first stage, the simulation and validation process described in Figure 1 was developed, thereby considering the operating parameters established in Tables 1–4. Next, a sensitivity analysis of the process was carried out to identify the input variables of the ANNs. Subsequently, the neural network was trained, validated, and tested using a simulation-based database. Finally, the effectiveness of the network was evaluated through statistical analyses and graphical representations, thus ensuring a deep and rigorous understanding of its performance. This methodological approach provides a solid foundation for the successful implementation of ANNs in predicting the studied process.

2.3. DWSIM simulation

DWSIM, an open-source chemical process simulator, can be utilized on various operating systems, including Windows, Linux, Android, macOS, and iOS. This software enables engineers to effectively construct process plants by leveraging rigorous thermodynamic principles and utilizing unit operations [16,17].

The distillation towers utilized for the simulation depicted in Figure 1 are by the "Chem-Sep Column" model. All flow streams are operated using the modified UNIFAC property package. Simultaneously, the DECHEMA/Modified UNIFAC/Antonie/Ideal thermodynamic models are adjusted for the distillation towers. These models enable the accurate depiction of the non-ideality of the liquid system through the calculation of activity coefficients of the liquid and the modeling of the vapor phase [2,18–21]. The conditions in Tables 2–4 align with the operating conditions employed during the process simulation.

Newton's method was the mathematical technique employed to ascertain the convergence of the simulation process, with an established maximum of 100 iterations.

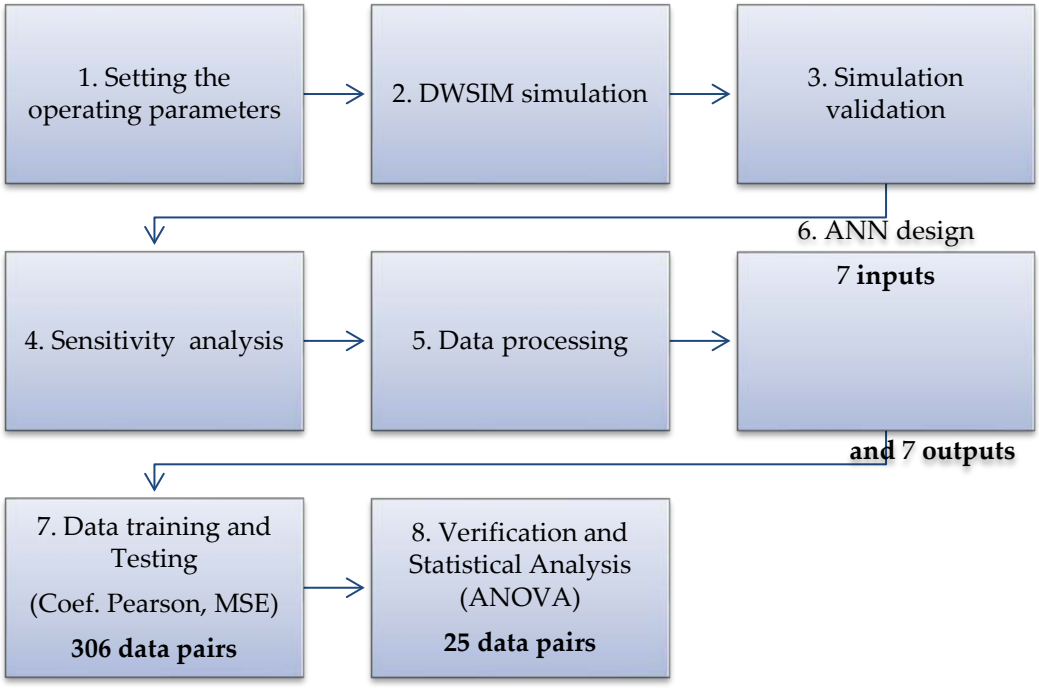

Figure 2. Methodological scheme of the designed ANN.

2.4. Sensitivity analysis

A sensitivity analysis is performed to ascertain the selection of the input and output variables in an ANN to assess the relative significance of these variables. It assists in identifying the most pertinent characteristics while eliminating irrelevant ones, optimizing the architecture, and diagnosing potential complications. To conduct this analysis, the possible manipulated variables were defined, thus establishing ranges of variation by the physical-chemical rationale of the actual process.

2.5. Design and training of the ANN

The training of the ANN involves adjusting the weights of the connections between neurons to enable the ANN to make accurate predictions about the targeted output data. The validation process is used to measure the prediction errors of the ANN, thereby assessing its performance. On the other hand, the testing phase involves evaluating the predictions made by the ANN using pairs of data that were not utilized during the training process [17].

The literature surrounding ANNs that useda minimum of 50 data points for predictive regression algorithms can be found in [22–24]. With this guidance, 306 data pairs were generated by introducing random variations to the operational parameters and by selecting performance indicators for this investigation.

Following the recommendations provided by Chen et al. [25], 70% of the complete dataset (consisting of 214 data sets) was utilized to train and learn the ANN. In comparison, the remaining 30% (comprising 92 data sets) were allocated for testing to evaluate the ANN's proficiency in learning.

2.6. ANN validation

To validate the ANN, we utilized a variety of performance metrics. These metrics included the mean square error (MSE), which measures the average squared difference between the predicted and actual values, and the regression coefficient (R), which quantifies the strength and direction of the linear relationship between the predicted and actual values. These metrics were defined by Eqs 1 and 2, respectively [26–28]. Additionally, we utilized an ANOVA to assess the ANN's performance further.

Moreover, we implemented an iterative process to fine-tune the ANN's performance. This iterative process aimed to minimize the MSE and enhance the correlation coefficients during the training, validation, and testing phases. By continuously adjusting the parameters of the ANN based on the performance evaluation, we aimed to optimize the network's ability to accurately predict the desired outcomes. Thus, this iterative process improved the ANN's effectiveness and reliability:

$$MSE = \frac{1}{n}\sum_{t=1}^{n}\left(y - y^{'}\right)^2 \tag{1}$$

$$R = \frac{n\sum_{i=1}^{n}(y'y) - [\sum_{i=1}^{n} y'][\sum_{i=1}^{n} y]}{\sqrt{[n\sum_{i=1}^{n} y^2 - [\sum_{i=1}^{n} y^2]\,[n\sum_{i=1}^{n} y'^2 - [\sum_{i=1}^{n} y'^2]}} \tag{2}$$

Where *n* is the number of observations, *y* are the actual results (simulation outputs), and *y'* are the predicted targets (ANN outputs).

3. Results and discussion

This section presents the analysis and discussion of the process simulation and the ANN's design, training, and validation.

3.1. Simulation validation

The validation process of the simulation in DWSIM involved comparing it with the study carried out in ASPEN PLUS by Chen et al. [29]. Table 5 was used to summarize the errors in the mass fractions of interest in their respective distillation columns. It is important to note that these errors do not exceed 5%. This particular error percentage can be justified by the presence of minute traces of other components in both the distillate stream and the background stream, which are considered to have a negligible impact.

Table 5. Simulation validation (mass fraction).

Column	Parameter	Aspen Plus Chen et al. [29]	DWSIM	Error (%)
CDC	DIB (bottom)	0.61	0.61	1.16
	DIM (bottom)	0.29	0.30	4.57
ADC	DIB (bottom)	0.65	0.66	1.71
	DIM (bottom)	0.31	0.32	3.19
	TBA (distillate)	0.94	0.92	1.93
TDC	DIB (distillate)	0.99	0.99	0.72
	DIM (bottom)	0.90	0.93	4.35

3.2. Sensitivity analysis

Critical variables affecting the products of interest were selected when modified in the reactive distillation, TBA recovery, and dimer separation steps. The sensitivity analyses to determine the variables that significantly impacted the target compounds are detailed in Appendix A. Table 6 shows the parameters that directly influenced obtaining high-purity components.

Table 6. ANN inputs and outputs.

ANN	Column	Nomenclature	Parameter	Units
Inputs	CDC	X_{IB}	Mass fraction of isobutylene in feed C4 -	-
		$X_{2\text{-}Bu}$	Mass fraction of 2-butene in feed C4 -	-
		T_{C4}	Feed temperature C4	ºC
		T_{TBA}	Feed temperature TBA	ºC
		P_{CDC}	CDC column operating pressure	atm
	ADC	P_{ADC}	ADC column operating pressure	atm
	TDC	P_{TDC}	Column operating pressure TDC	atm
Outputs	CDC	X_{DIB}	Mass fraction of DIB in the Bottom-CDC	-
		X_{DIM}	Mass fraction of DIM in the Bottom-CDC	-
	ADC	X_{DIB}	Mass fraction of DIB in the Bottom-ADC	-
		X_{DIM}	Mass fraction of DIM in Bottom-ADC	-
		X_{TBA}	Mass fraction of TBA in Distillate-ADC	-
	TDC	$X_{DIB\text{-}TOP}$	Mass fraction of DIB in the Distillate-TDC	-
		$X_{DIM\text{-}BOTTOM}$	Mass fraction of DIM in Bottom-TDC	-

Table 7 shows the variation of the inputs chosen based on typical and extreme operation ranges.

Table 7. ANN input's restrictions.

Column	Parameter	Nomenclature	Range	Units
CDC	Mass fraction of isobutylene in feed C4 -	X_{IB}	0.07–0.86	-
	Mass fraction of 2-butene in feed C4 -	$X_{2\text{-}Bu}$	0.02–0.81	-
	Feed temperature C4	T_{C4}	10–40	ºC
	Feed temperature TBA	T_{TBA}	10–35	ºC
	CDC column operating pressure	P_{CDC}	8–15	atm
ADC	ADC column operating pressure	P_{ADC}	5–10	atm
TDC	Column operating pressure TDC	P_{TDC}	0.01–0.99	atm

3.3. Design and training of the ANN

The design of the ANN (Figure 3) is based on seven input parameters: IB mass fraction in C4, 2-butene mass fraction in C4, feed temperature C4, feed temperature TBA, CDC column pressure, ADC column pressure, and TDC column pressure. These input variables were chosen due to their importance in the final products' quality and optimization processes. Seven output parameters were considered: mass fraction of DIB and DIM in the residue of the CDC column, mass fraction of DIB and DIM in the residue and mass fraction TBA in the distillate of the ADC column, mass fraction DIB in the distillate, and molar fraction of DIM in the residue of the TDC column.

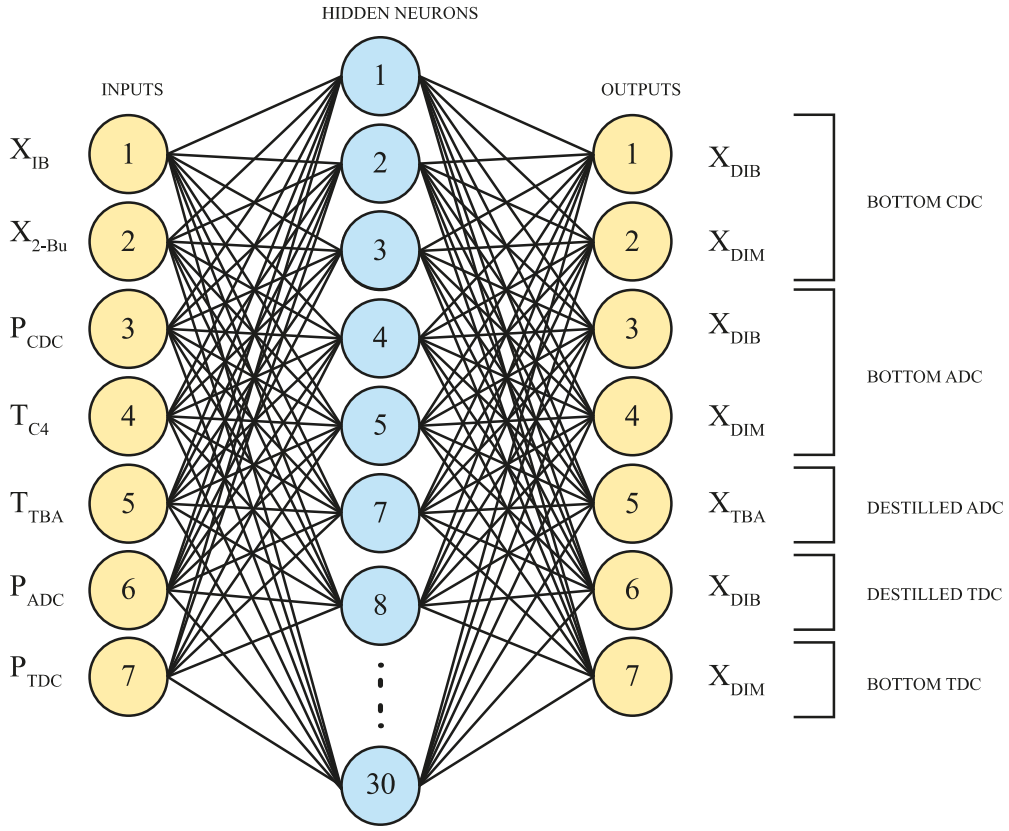

Figure 3. Schematic of the designed ANN.

3.4. ANN topology

This section describes the design and structuring of the ANN by analyzing the correlation coefficient (R) and the MSE.

3.4.1. Selection of ANN training algorithm

The ANN architecture employed in this study used three training algorithms that have been previously demonstrated to be effective in minimizing the MSE loss function: the Levenberg-Marquardt (LM), Bayesian regularization (BR), and scaled conjugate gradient back-propagation (SCG) algorithms. These training techniques surpass many other commonly utilized algorithms by more effectively converging towards solutions with lower MSE values, as the literature on optimization approaches for neural networks indicates [30–32].

The performance of the three training algorithms was assessed through R and MSE metrics, as observed in Table 8, which is similar to other studies in predictive modeling [33,34]. The number of neurons was systematically altered to determine the impact of the architectural choice of the hidden layer. This variation allowed us to evaluate the model's accuracy across different optimization approaches. Consequently, a comparison of the robustness and sensitivity of the algorithms to tuning parameters was made possible.

Table 8. Pearson's correlation coefficient (*R*) and mean square error (MSE) values for trial and error using Levenberg–Marquardt (LM), Bayesian regularization (BR), and scaled conjugate gradient back-propagation (SCG) algorithms.

# hidden	LM		BR		SCG	
neurons	*R* Global	*MSE*	*R* Global	*MSE*	*R* Global	*MSE*
10	0.902	0.024	0.907	0.023	0.890	0.026
20	0.917	0.020	0.917	0.021	0.867	0.031
30	0.930	0.006	0.986	0.011	0.486	0.033
35	0.897	0.023	0.944	0.013	0.853	0.027
40	0.898	0.025	0.943	0.039	0.880	0.029
50	0.921	0.020	0.939	0.028	0.893	0.025
60	0.956	0.008	0.924	0.020	0.894	0.027
70	0.919	0.028	0.901	0.030	0.952	0.008
80	0.904	0.024	0.815	0.007	0.870	2.049
90	0.919	0.020	0.915	0.024	0.888	0.025
100	0.913	0.022	0.893	0.032	0.890	0.027

The results of the training procedure elucidated in Table 8 illustrate that the BR algorithm generated the most precise and dependable model for foretelling the target outputs, with an MSE of 0.011 and the maximum R-value of 0.986. As pointed out in preceding research [30,35,36], the BR's pivotal advantage is its ability to unveil intricate associations within data to produce less prejudiced decisions.

Although computationally more expensive than other techniques, BR has demonstrated its ability to produce robust generalizations from small, noisy, or complex datasets, thus surpassing the performance of methods such as Levenberg-Marquardt. This particular strength in modeling potential

nonlinear effects, even in limited data samples, renders BR as highly suitable for quantitative analyses that necessitate an accurate and reliable predictive performance [30]. By harnessing the capabilities of BR, the constructed model establishes a solid basis to extract insights from the empirical data gathered.

3.4.2. Selection of the number of neurons in the hidden layer

Determining the optimal neuron's number helps conduct trials to determine the required local minimum in the error surface and oscillations in R.

The analysis presented in Table 9 demonstrates that 30 neurons yield the most significant R-values during the testing phase. Specifically, the R-value obtained during testing reached an impressive 0.934, while the MSE values were recorded at 0.011. Upon observing the maximum R-value and minimum MSE, these findings strongly imply that this hidden layer's optimal number of neurons is 30. Furthermore, the combination of higher R-values and lower error rates observed with 30 neurons indicates that it provided the best model performance.

Table 9. *R* and *MSE* values for determining the optimal number of neurons in the hidden layer using BR.

# hidden neurons	*R* Training	*R* Testing	*R* Global	*MSE*
10	0.925	0.888	0.907	0.023
20	0.949	0.885	0.917	0.021
30	0.995	0.934	0.986	0.011
35	0.978	0.910	0.944	0.013
40	0.978	0.908	0.943	0.039

The present study involved the construction of an ANN model that employed MATLAB NNTOOL R2018a. After careful examination, the ANN architecture was determined to be comprised of seven input neurons a singular hidden layer of 30 neurons. It was determined to be the optimal choice with seven output neurons. Previous investigations into predictive modeling have consistently indicated that including one hidden layer is often adequate to facilitate precise forecasts across various ANN applications. [17,37].

3.4.3. ANN training and testing

Table 10 presents the MSE values for the ANN training and testing phases. However, there are no results available for the validation phase. This absence of results can be justified using the BR algorithm in the ANNs. This algorithm increases the robustness of the models and diminishes or even eliminates the necessity of validation. Consequently, the data collected during training is effectively exploited. The MSE values for the training and testing phases exhibit values of 0.0008 and 0.0212, respectively, thus indicating the satisfactory functionality of the ANN and its ability to generate predictions with a desirable level of accuracy. In Figure 4, the progressive behavior of the MSE is exhibited throughout the training phase, thus culminating in a final value of 0.0008251. The performance of the MSE function for the training data (train) is almost zero, which indicates the network's exceptional predictive capability.

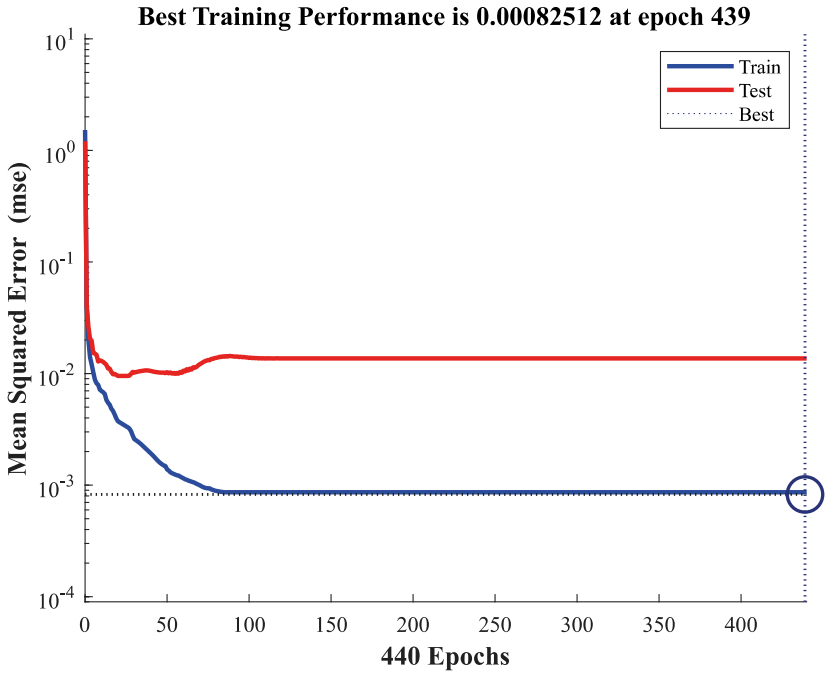

Figure 4. ANN training performance (*MSE*).

Table 10. The mean square error of ANN designed.

PHASE	*MSE*
Train performance (training)	0.0008
Test performance (testing)	0.0212

Figure 5 illustrates the R values obtained during the training and testing phases. Specifically, the R-values obtained for training and testing were 0.995 and 0.934, respectively. Additionally, the overall R-value was determined to be 0.983. These noteworthy R-values satisfactorily correlate between the predicted outputs and the desired targets. In general, R-values that approached 1 indicated the enhanced performance of the ANN. Specific benchmarks were established to confirm the ANN's effectiveness, including R-values ranging from 0.95 to 1 and an MSE below 0.025. Meeting these criteria substantiates that the developed ANN is a dependable and precise predictive model for the given application.

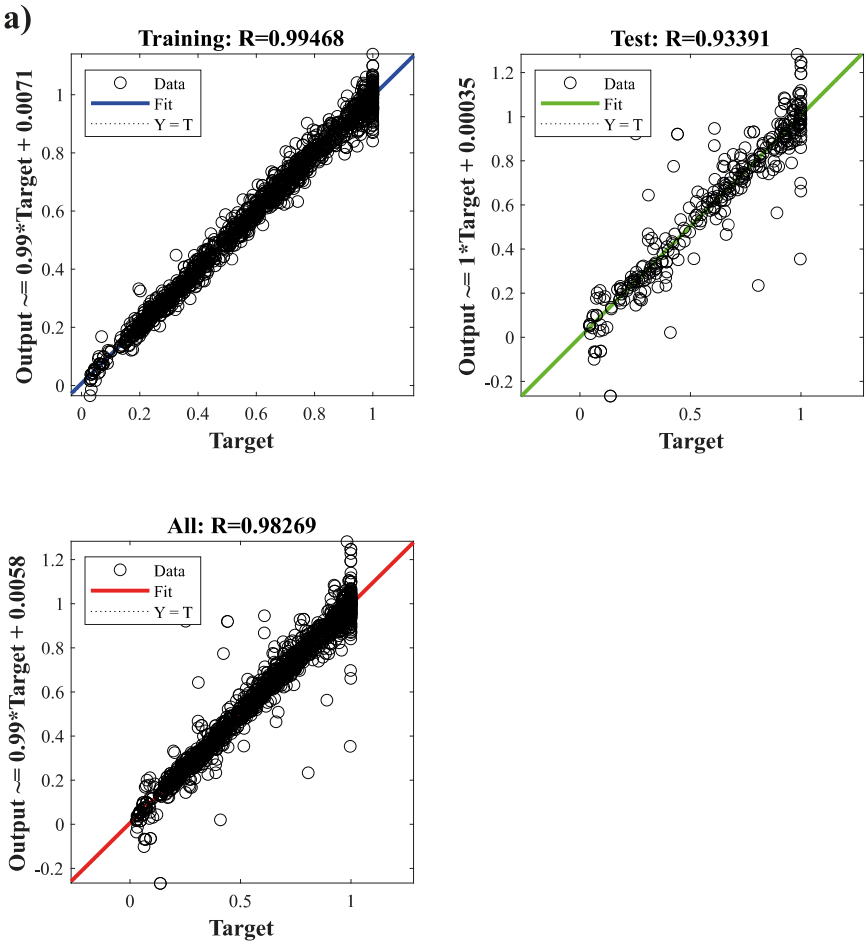

Figure 5. Regression coefficient *R* for the ANN.

3.5. Model prediction of DIB, DIM, and TBA in CDC – Catalytic distillation column, ADC – TBA recovery column, and TDC – Vacuum distillation column for separating isomers.

Figures 6–12 show the overlap between experimental values (obtained by simulation) and predictions (obtained by ANN) in the reactive, recovery, and vacuum columns, respectively. The comparisons obtained in the three columns are relatively equal. The developed model is close to the experimental data, thus demonstrating that ANNs constitute a robust and suitable model to predict the DIB, DIM, and TBA concentrations, and that it can be applied in IB dimerization processes in crude oil distillation processes to obtain and concentrate DIB.

Based on the analysis of Figures 6–12, the average percentage error (%E) of the predictions is as follows: 6.05% (DIB in the residue) and 7.27% (DIM in the residue) in the reactive column (CDC); 5.68 (DIB in the residue), 9.55% (DIM in the residue), and 6.4% (TBA in the distillate) in the recovery column (ADC); and 4.4% (DIB in the distillate) and 5% (DIM in the residue) in the vacuum column (TDC).

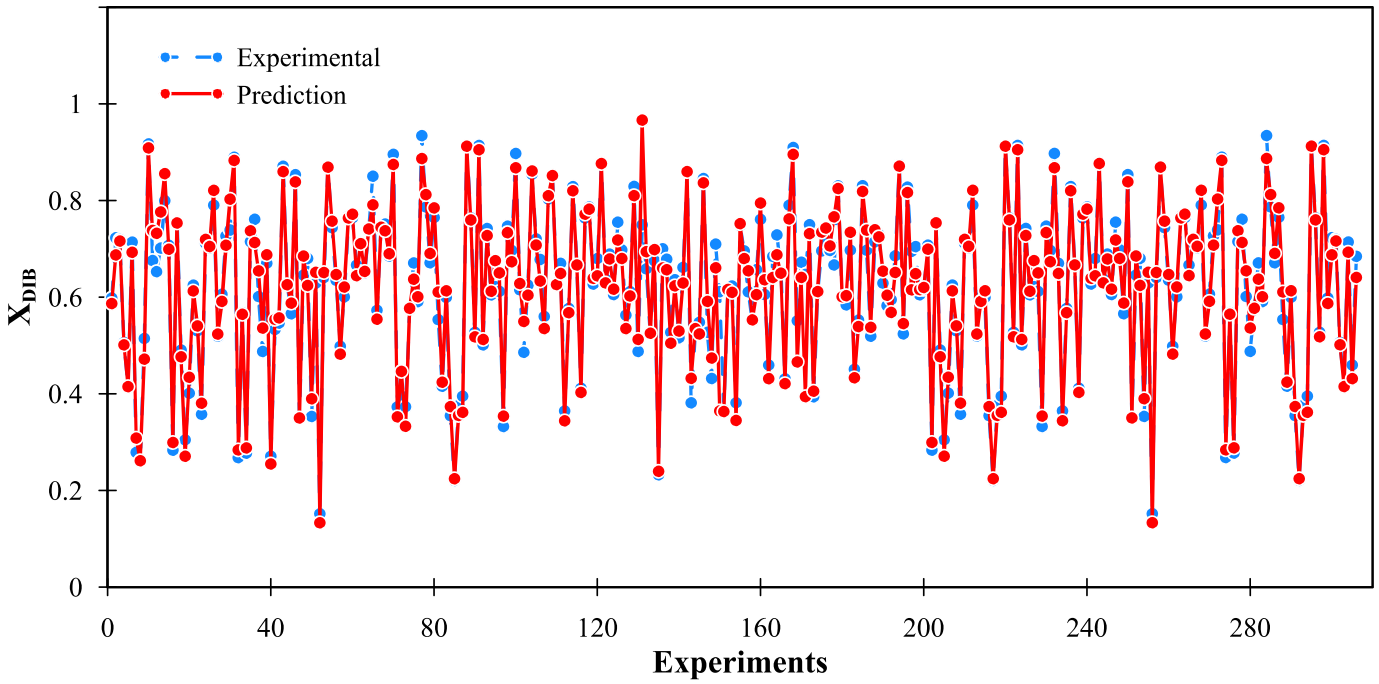

Figure 6. DWSIM (Experimental) and ANN (prediction) results at the bottom of the EDC (X_{DIB}).

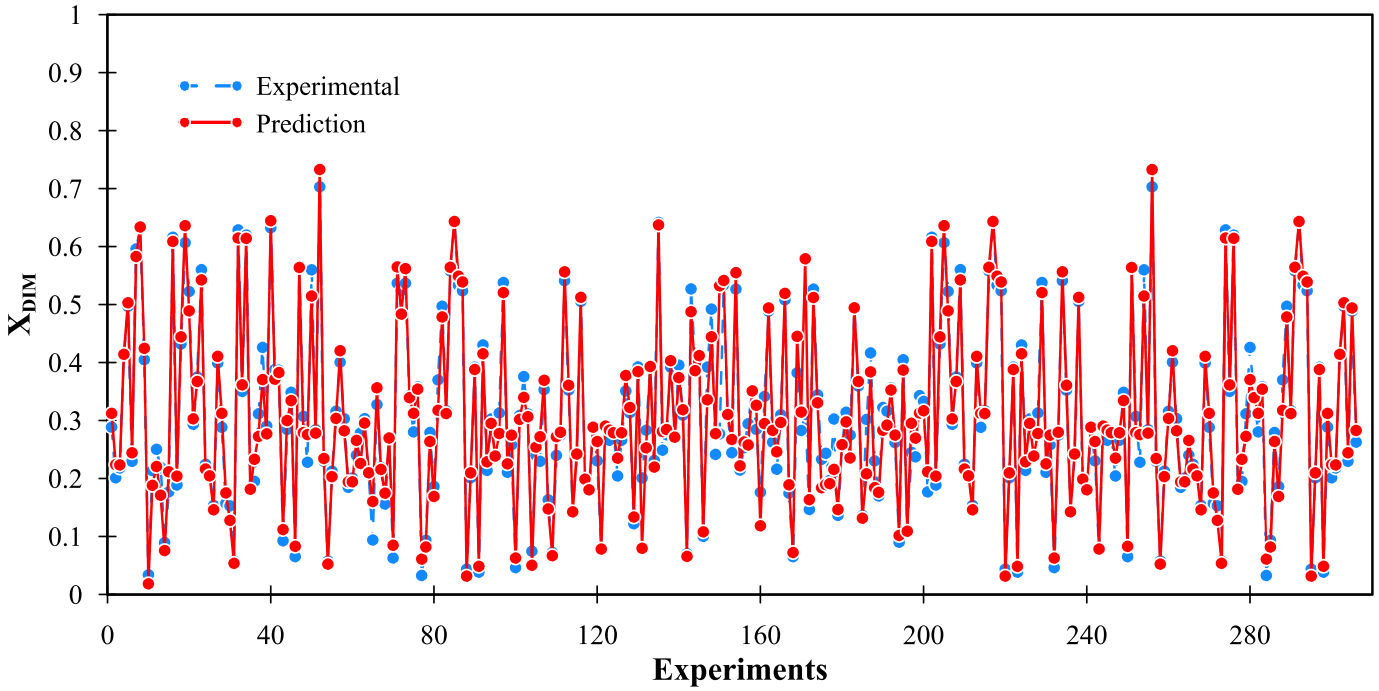

Figure 7. DWSIM (Experimental) and ANN (prediction) results at the bottom of the EDC (X_{DIM}).

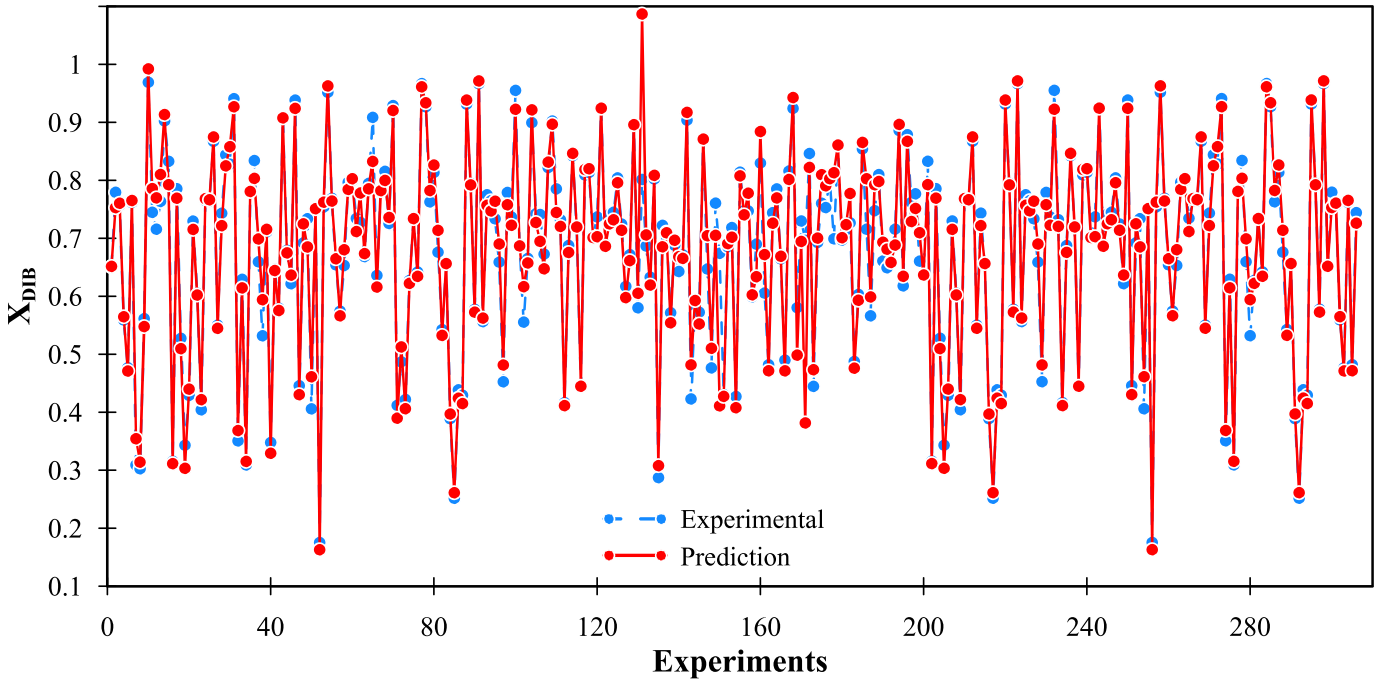

Figure 8. DWSIM (Experimental) and ANN (prediction) results at the bottom of the ADC distillate (X_{DIB}).

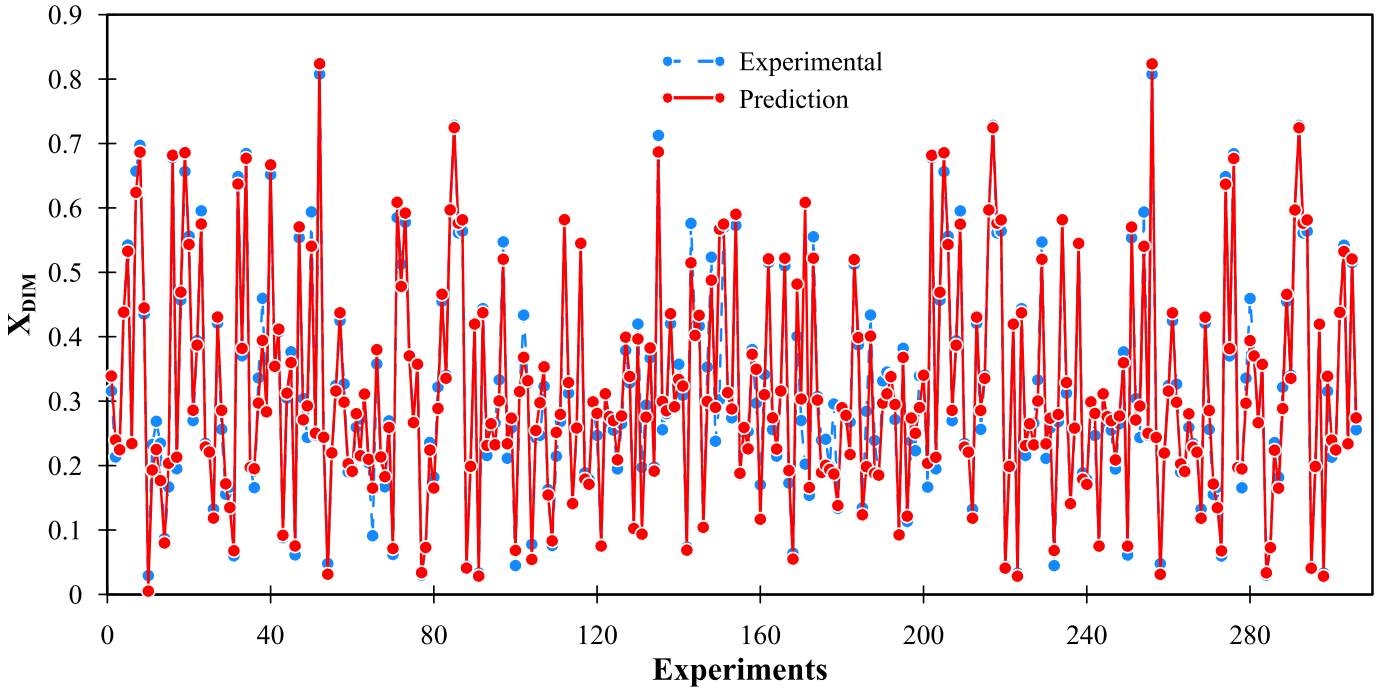

Figure 9. DWSIM (Experimental) and ANN (prediction) results at the bottom of the ADC (X_{DIM}).

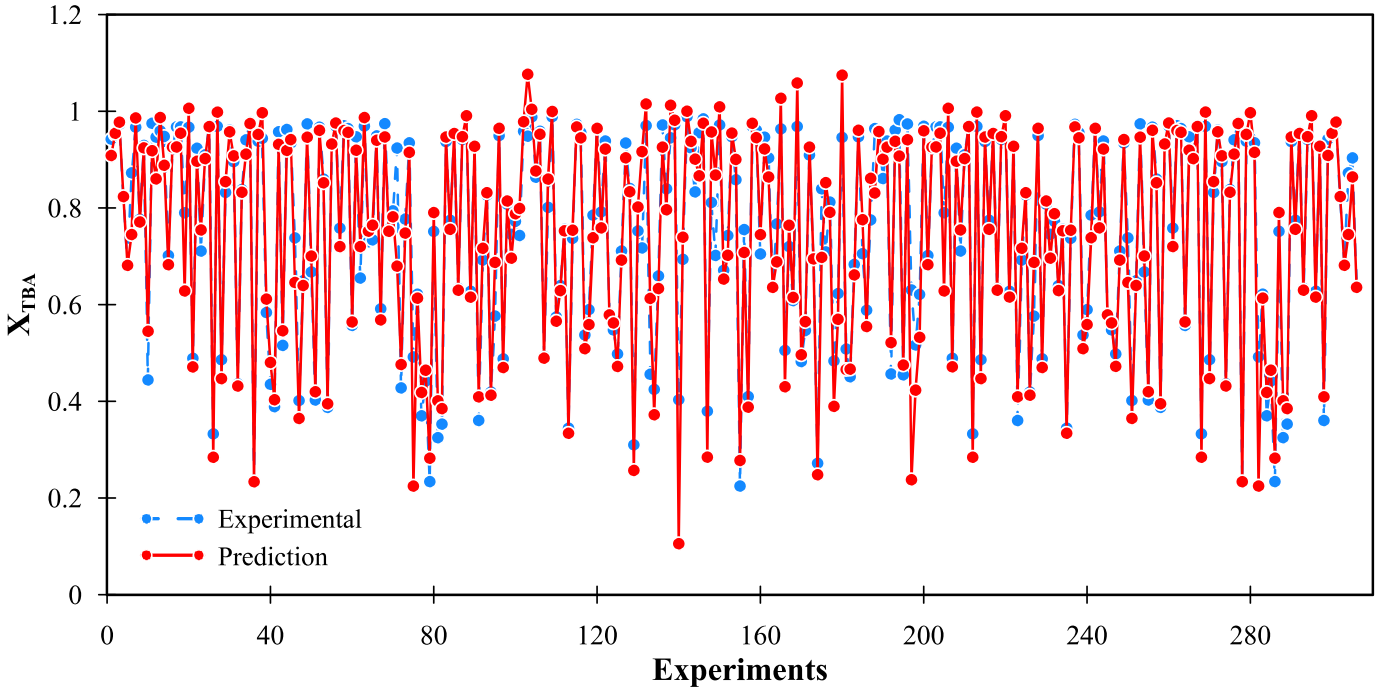

Figure 10. DWSIM (Experimental) and ANN (prediction) results at the distillate of the ADC (X_{TBA}).

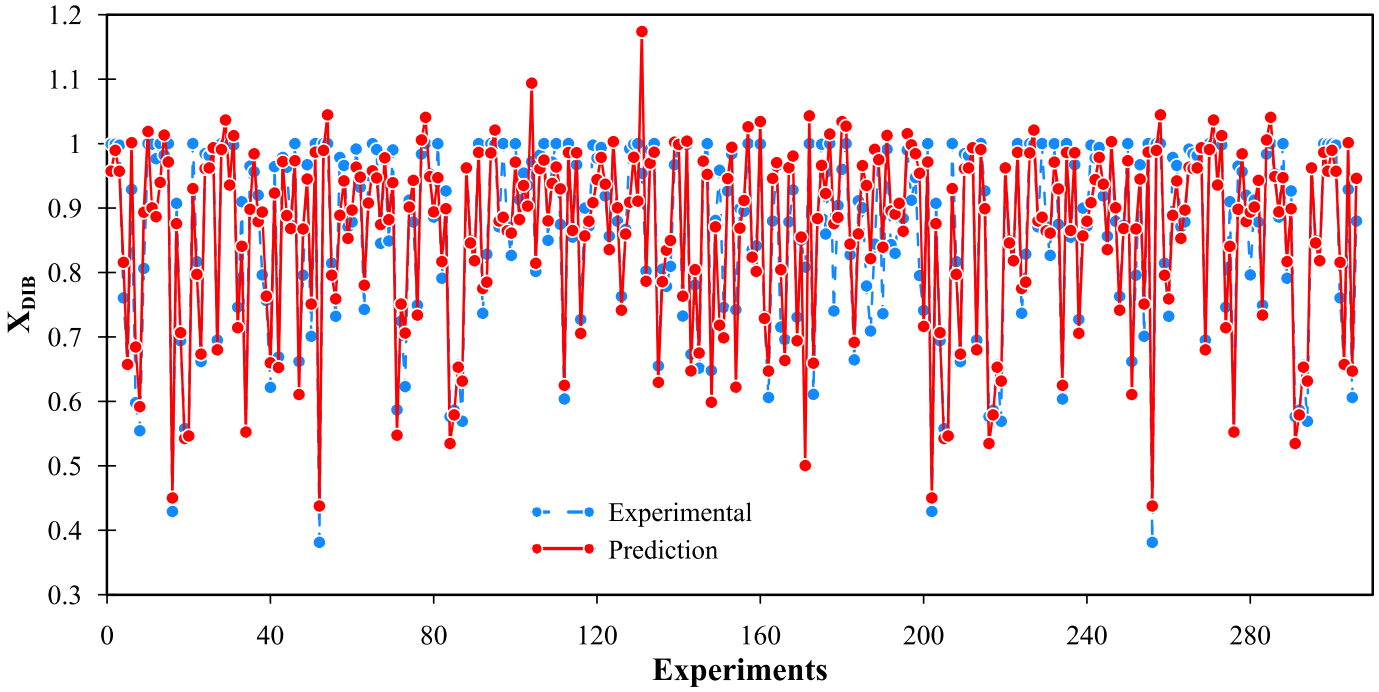

Figure 11. DWSIM (Experimental) and ANN (prediction) results at the distillate of the TDC (X_{DIB}).

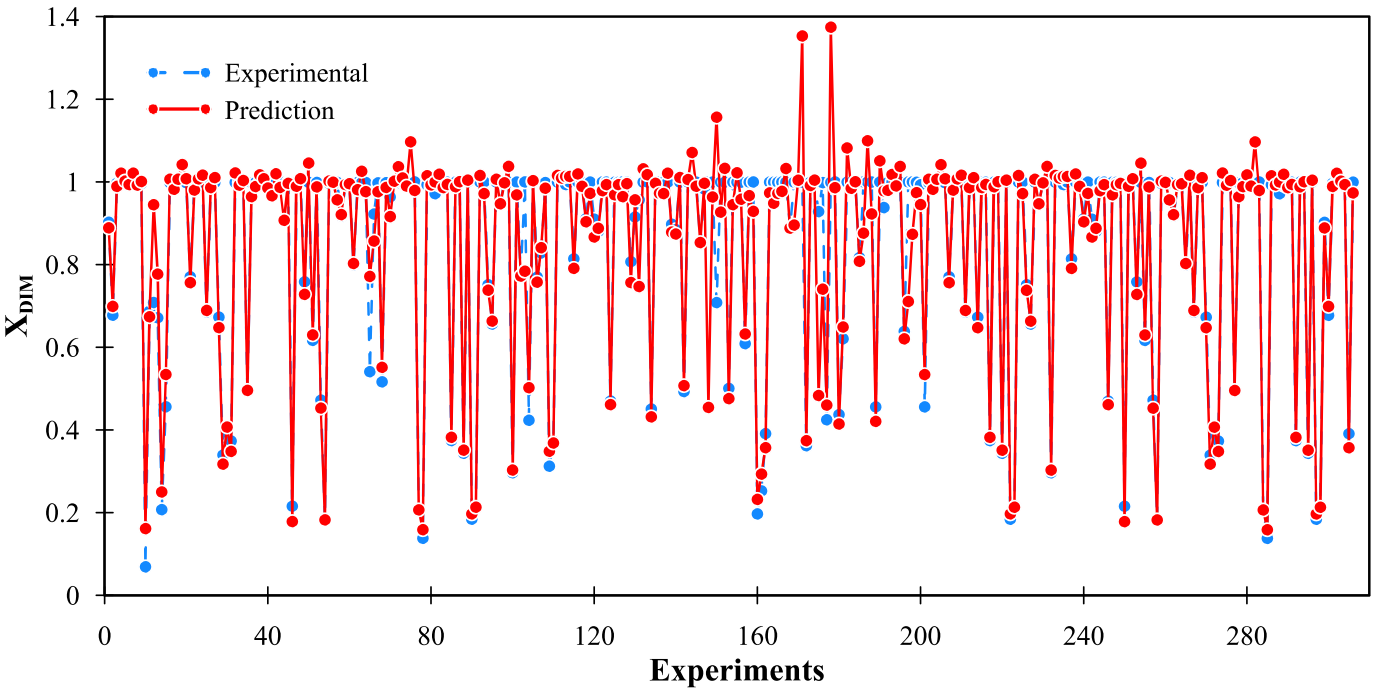

Figure 12. DWSIM (Experimental) and ANN (prediction) results at the bottom of the TDC (X_{DIM}).

3.6. ANN model verification

The predictive ability of the ANN of the concentration of DIB, DIM, and TBA in the reagent, recovery, and vacuum column was tested with a set of 25 random input data ([IB],[2-Bu], P_{CDC}, T_{C4}, T_{TBA}, P_{ADC} and P_{TDC}) unknown to the ANN. The results show an overlap between the experimental data and the predictions. This indicates that the ANN has an excellent predictive capacity for the mass fractions of distillates and residues from distillation columns (Figure 13).

This research uses the ANOVA functions [32] using SPSS 22.0 to statistically validate the ANN. Table 11 shows the results of the ANOVA, and for all cases, the P values (probability value in statistical significance tests) are more significant than 0.05, thus indicating no statistically significant difference between the means of the observations and the predictions. These statistical tests reveal that the constructed ANN is statistically valid to predict the mass fractions of DIB, DIM, and TBA in EDC, ADC, and TDC columns, with a confidence level of 95%.

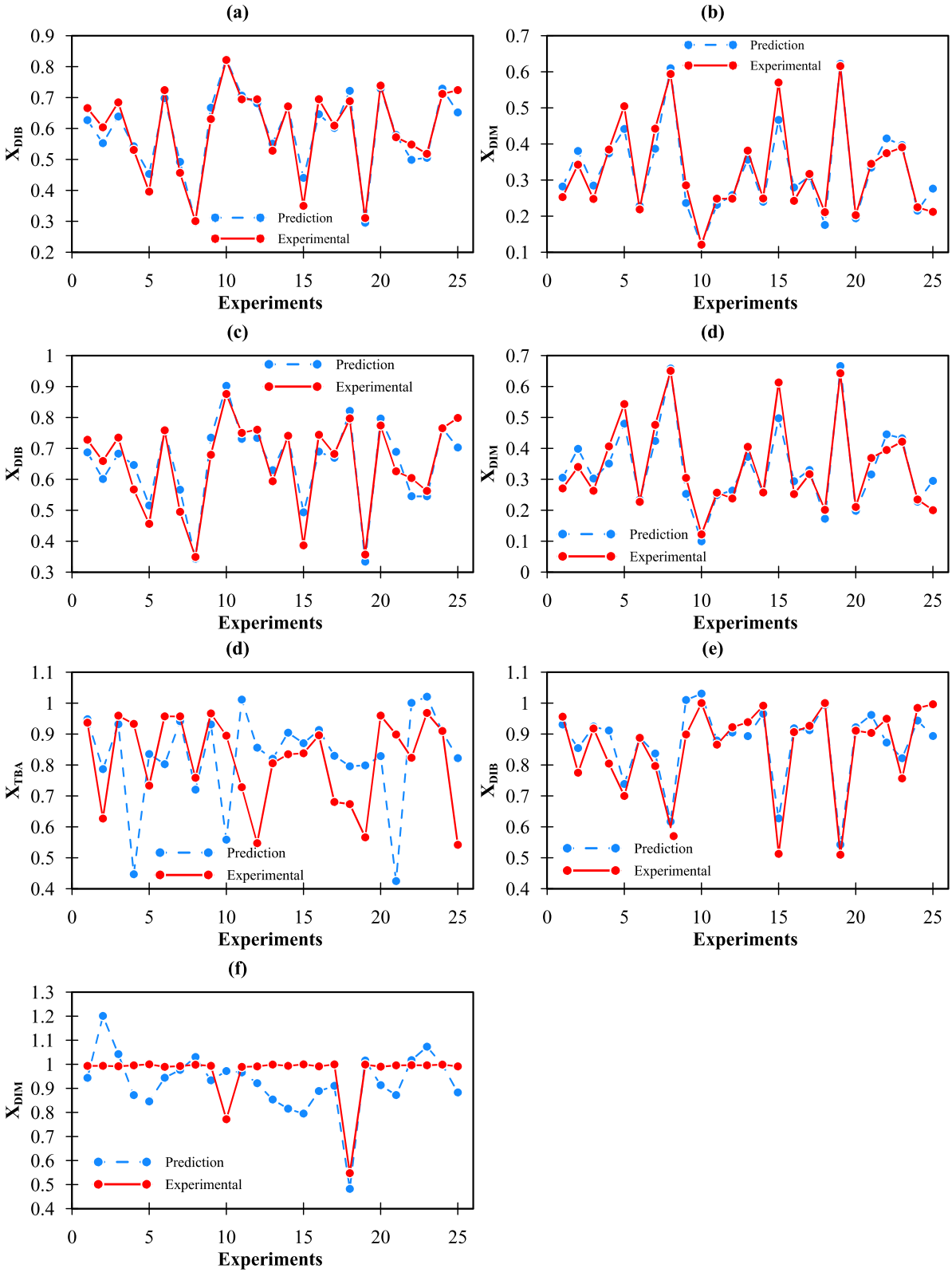

Figure 13. Comparison between experimental and predictions data - EDC: a) X_{DIB} (bottom-EDC), b) X_{DIM} (bottoms-EDC), c) X_{DIB} (bottoms-ADC), d) X_{DIM} (bottoms-ADC), e) X_{TBA} (distillate-ADC), f) X_{DIB} (bottom- TDC), g) X_{DIM} (bottom-TDC).

Table 11. ANOVA.

Source	Sum of squares	DOF	Mean square	*F*-Value	*P*-value
X_{DIB} in EDC bottoms					
Inter groups	0.0000	1	0.0000	0.01	0.943
Intra groups	0.8930	48	0.0186		
Total (Corr.)	0.8931	49			
X_{DIM} in EDC bottoms					
Inter groups	0.0002	1	0.0002	0.01	0.903
Intra groups	0.7839	48	0.0163		
Total (Corr.)	0.7842	49			
X_{DIB} in ADC bottoms					
Inter groups	0.0001	1	0.0001	0.01	0.936
Intra groups	0.9629	48	0.0200		
Total (Corr.)	0.9630	49			
X_{DIM} in ADC bottoms					
Inter groups	0.0001	1	0.0001	0.01	0.923
Intra groups	0.9616	48	0.0200		
Total (Corr.)	0.9618	49			
X_{TBA} in ADC distillate					
Inter groups	0.0019	1	0.0019	0.09	0.767
Intra groups	1.0542	48	0.0219		
Total (Corr.)	1.0562	49			
X_{DIB} in TDC bottoms					
Inter groups	0.0029	1	0.0029	0.17	0.682
Intra groups	0.8490	48	0.0176		
Total (Corr.)	0.8520	49			
X_{DIM} in TDC bottoms					
Inter groups	0.1015	1	0.1015	3.53	0.066
Intra groups	1.3806	48	0.0287		
Total (Corr.)	1.4821	49			

3.7. Benefits of using ANNs for process optimization and energy environment assessment

ANNs can optimize parameters such as temperature, pressure, flow rates, and reactant concentrations to maximize the industrial processes' performance and efficiency. In addition, it allows you to minimize resources and increase the system productivity.

On the other hand, ANNs allow you to analyze the energy consumption through a historical analysis of consumption data and subsequently predict the energy consumption patterns, thus allowing you to efficiently manage the energy consumption and minimize expenses.

In addition, ANNs can be designed and/or reprogrammed to evaluate and minimize the environmental impacts generated in the industry by predicting the emissions and dispersion of pollutants to reduce the carbon footprints. This becomes important when complying with environmental regulation standards and ensuring the sustainability of an industry in the short and long term.

Finally, ANNs can be coupled to a plant process through a SCADA system to make quick and effective real-time decisions.

Figure 14 presents a generalized diagram of the steps and actions necessary to implement the ANN in the industrial process. The following recommendations are suggested to implement the ANN in real-time: define the objectives of the ANN (quality control or process optimization); define the historical database for re-training the ANN; preprocess the database; train the ANN; implement the ANN in hardware integrated into the automatic process control system; implement the real-time ANN performance monitoring mechanisms; periodically update the ANN through feedback loops for the continuous improvement of the ANN; implement security measures based on the predictions made by the ANN; and document the entire process.

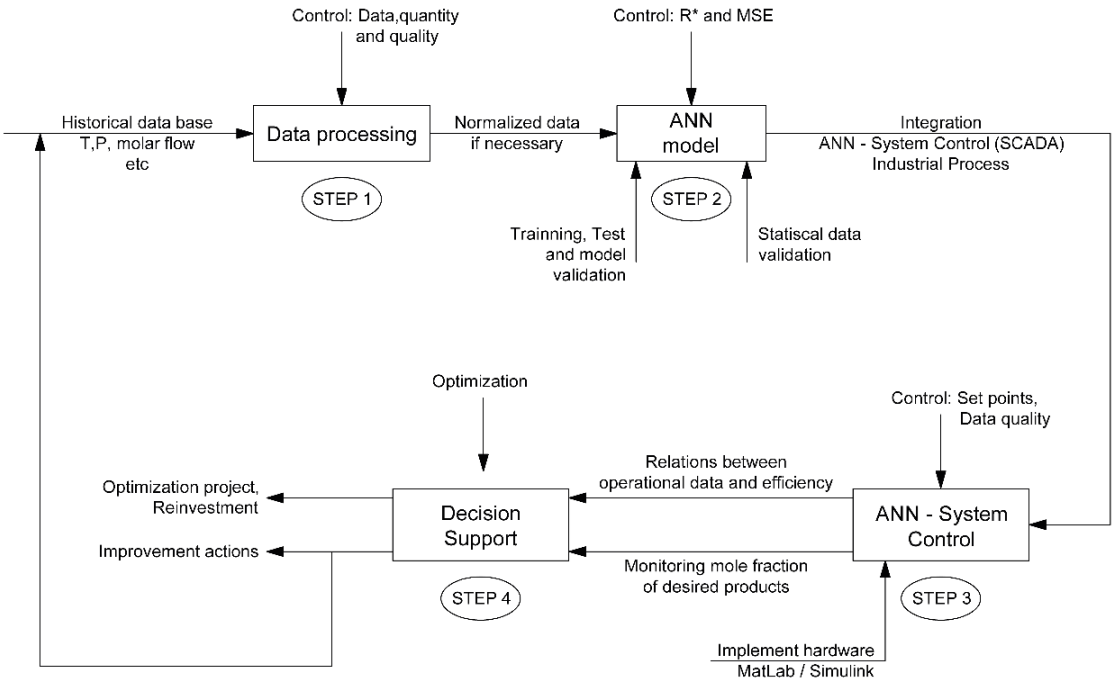

Figure 14. Generalized diagram to implement the ANN.

4. Conclusions

In this study, the mass fractions of an IB dimerization system with DIB-DIM-TBA azeotrope separation were predicted using an ANN based on the process simulation in DWSIM. The developed ANN had 30 hidden neurons and was trained with a base of 306 data pairs with seven input variables (neurons): IB mass fraction, 2-butene mass fraction, CDC column pressure, C4 feed temperature, TBA feed temperature, pressure ADC column, and TDC column pressure. It can predict seven output variables (neurons): the mass fraction of DIB and DIM in the residue of the CDC column, the mass fraction of DIB and DIM in the residue, the mass fraction of TBA in the distillate of the ADC column, the mass fraction of DIB in the distillate and the mass fraction of DIM in the residue of the TDC column.

The Bayesian regularization approach was used to train the ANN, which had an MSE of 0.011 and a total R of 0.986. Additionally, an ANOVA between the data (DWSIM) and the values predicted by the neural network was used to validate the ANN. Statistical tests showed that the ANN accurately predicted the mass fractions in the outputs with a 95% significance level.

According to the findings, the ANN developed in this work can be used as a prediction tool to improve IB dimerization processes in the FCC-C4 waste stream from the crude oil distillation process. For example, accurate operating parameters of the described process must be used as the input, applied in situ, and the predictions should be verified at the control points (ANN outputs). Subsequently, when validated in the plant and coupled to the existing control process, the energy and environmental optimization of the process can be promoted by connecting genetic optimization algorithms to the network (hybrid technologies). Optimization studies in an actual plant will be the subject of future research.

Use of AI tools declaration

The authors declare they have not used Artificial Intelligence (AI) tools in creating this article.

Acknowledgments

The authors thank the Security Research Group on Environment and Engineering, “GISAI” for allowing the execution of this research.

Conflict of Interest

The authors declare no conflict of interest.

References

1. Honkela ML, Krause AOI (2003) Influence of polar components in the dimerization of isobutene. *Catalysis Letters* 87: 113–119. https://doi.org/10.1023/A:1023478703266
2. Chen Z, Zhang Z, Zhou J, et al. (2021) Efficient synthesis of isobutylene dimerization by catalytic distillation with advanced heat-integrated technology. *Ind Eng Chem Res* 60: 6121–6136. https://doi.org/10.1021/acs.iecr.1c00945
3. Liu J, Ding N, Ge Y, et al. (2019) Dimerization of Isobutene in C4 mixtures in the presence of ethanol over acid ion-exchange resin DH-2. *Catal Letters 149*: 1277–1285. https://doi.org/10.1007/s10562-019-02685-y
4. Talwalkar S, Mankar S, Katariya A, et al. (2007) Selectivity engineering with reactive distillation for dimerization of C 4 Olefins: Experimental and theoretical studies. *Ind Eng Chem Res* 46: 3024–3034. https://doi.org/10.1021/ie060860+
5. Kamath RS, Qi Z, Sundmacher K, et al. (2006) Process analysis for dimerization of isobutene by reactive distillation. *Ind Eng Chem Res* 45: 1575–1582. https://doi.org/10.1021/ie0506522

6. Kamath RS, Qi Z, Sundmacher K, et al. (2006) Comparison of reactive distillation with process alternatives for the isobutene dimerization reaction. *Ind Eng Chem Res* 45: 2707–2714. https://doi.org/10.1021/ie051103z
7. Goortani BM, Gaurav A, Deshpande A, et al. (2015) Production of isooctane from isobutene: Energy integration and carbon dioxide abatement via catalytic distillation. *Ind Eng Chem Res* 54: 3570–3581. https://doi.org/10.1021/ie5032056
8. Chalakova M, Kaur R, Freund H, et al. (2007) Innovative reactive distillation process for the production of the MTBE substitute isooctane from isobutene. *DGMK/SCI-Conference.* Available from: https://www.osti.gov/etdeweb/servlets/purl/21074149
9. Zhang L, Sun X, Gao S (2022) Temperature prediction and analysis based on improved GA-BP neural network. *AIMS Environ Sci* 9: 735–753. https://doi.org/10.3934/environsci.2022042
10. Nualtong K, Chinram R, Khwanmuang P, et al. (2021) An efficiency dynamic seasonal regression forecasting technique for high variation of water level in yom river basin of thailand. *AIMS Environ Sci* 8: 283–303. https://doi.org/10.3934/environsci.2021019
11. Suphawan K, Chaisee K (2021) Gaussian process regression for predicting water quality index: A case study on ping river basin, thailand. *AIMS Environ Sci* 8: 268–282. https://doi.org/10.3934/environsci.2021018
12. Zhang Z, Zhao J (2017) A deep belief network based fault diagnosis model for complex chemical processes. *Comput Chem Eng* 107: 395–407. https://doi.org/10.1016/j.compchemeng.2017.02.041
13. Chouai A, Laugier S, Richon D (2002) Modeling of thermodynamic properties using neural networks: Application to refrigerants. *Fluid Phase Equilib* 199: 53–62. https://doi.org/10.1016/S0378-3812(01)00801-9
14. Manssouri I, Boudebbouz B, Boudad B (2021) Using artificial neural networks of the type extreme learning machine for the modelling and prediction of the temperature in the head the column. Case of a C6H11-CH3distillation column. *Materials Today Proceedings* 45: 7444–7449. https://doi.org/10.1016/j.matpr.2021.01.920
15. Alhajree I, Zahedi G, Manan ZA, et al. (2011) Modeling and optimization of an industrial hydrocracker plant. *J Pet Sci Eng* 78: 627–636. https://doi.org/10.1016/j.petrol.2011.07.019
16. DWSIM (2020) DWSIM – The Open Source Chemical Process Simulator. Available from: https://dwsim.org
17. Chuquin-Vasco D, Parra F, Chuquin-Vasco N, et al. (2021) Prediction of methanol production in a carbon dioxide hydrogenation plant using neural networks. *Energies* 14: 1–18. https://doi.org/10.3390/en14133965
18. Dimian AC, Bildea CS, Kiss AA (2014) Introduction in process simulation, In Dimian. *Integrated Design and Simulation of Chemical Processes* 2 Eds., Amsterdam: Elsevier, 35–71. https://doi.org/10.1016/B978-0-444-62700-1.00002-4
19. Kiss A (2013) Advanced distillation technologies - Design, control and applications. 1 Eds., Noida, India:Wiley. https://doi.org/10.1002/9781118543702
20. Soave G, Gamba S, Pellegrini L (2010) SRK equation of state: predicting binary interaction parameters of hydrocarbons and related compounds. *Fluid Phase* 299: 285–293. https://doi.org/10.1016/j.fluid.2010.09.012

21. Feng Z, Shen W, Rangaiah GP, et al. (2020) Design and control of vapor recompression assisted extractive distillation for separating n-hexane and ethyl acetate. *Sep Purif Technol* 240: 116655. https://doi.org/10.1016/j.seppur.2020.116655
22. Singh V, Gupta I, Gupta HO (2005) ANN based estimator for distillation - Inferential control. *Chem Eng Proces* 44: 785–795. https://doi.org/10.1016/j.cep.2004.08.010
23. Pedregosa F, Varaquaux G, Gramfort A, et al. (2011) Scikit-learn:machine learning in Python. J Mach Lear Res. Available from: https://www.jmlr.org/papers/volume12/pedregosa11a/pedregosa11a.pdf
24. Bloice M, Holzinger A (2016) A tutorial on machine learning and data science tools with python. *Lect Not Comp Sci* 9605: 435–480. https://doi.org/10.1007/978-3-319-50478-0_22
25. Chen Y, Song L, Liu Y, et al. (2020) A review of the artificial neural network models for water quality prediction. *Appl Sci* 10: 5776. https://doi.org/10.3390/app10175776
26. Zhang L, Sun X, Gao S (2022) Temperature prediction and analysis based on improved GA-BP neural network. *AIMS Environ Sci* 9: 735–753. https://doi.org/10.3934/environsci.2022042
27. Wang L, Wu B, Zhu Q, et al. (2020) Forecasting Monthly Tourism Demand Using Enhanced Backpropagation Neural Network. *Neural Process Lett* 52: 2607–2636. https://doi.org/10.1007/s11063-020-10363-z
28. Suphawan K, Chaisee K (2021) Gaussian process regression for predicting water quality index: A case study on ping river basin, thailand. *AIMS Environ Sci* 8: 268–282. https://doi.org/10.3934/environsci.2021018
29. Chen Z, Zhang Z, Zhou J, et al. (2021) Efficient synthesis of isobutylene dimerization by catalytic distillation with advanced heat-integrated technology. *Ind Eng Chem Res* 60: 6121–6136. https://doi.org/10.1021/acs.iecr.1c00945
30. Kayri M (2016) Predictive abilities of Bayesian regularization and levenberg-marquardt algorithms in artificial neural networks: A comparative empirical study on social data. *Math Comp Appl* 21: 20. https://doi.org/10.3390/mca21020020
31. Bharati S, Rahman M, Podder P, et al. (2019) Comparative Performance Analysis of Neural Network Base Training Algorithm and Neuro-Fuzzy System with SOM for the Purpose of Prediction of the Features of Superconductors. In: Abraham, A., Siarry, P., Ma, K., Kaklauskas, A. (eds) *Intelligent Systems Design and Applications. ISDA 2019. Advances in Intelligent Systems and Computing* 1181. https://doi.org/10.1007/978-3-030-49342-4_7
32. Saini LM (2008) Peak load forecasting using Bayesian regularization, Resilient and adaptive backpropagation learning based artificial neural networks. *Elec Pow Syst Res* 78: 1302–1310. https://doi.org/10.1016/j.epsr.2007.11.003
33. Wang L, Wu B, Zhu Q, et al. (2020) Forecasting Monthly Tourism Demand Using Enhanced Backpropagation Neural Network. *Neural Process Lett* 52: 2607–2636. https://doi.org/10.1007/s11063-020-10363-z
34. Zeng YR, Zeng Y, Choi B, et al. (2017) Multifactor-influenced energy consumption forecasting using enhanced back-propagation neural network. *Energy* 127: 381–396. https://doi.org/10.1016/j.energy.2017.03.094

35. Suliman A, Omarov B (2018) Applying Bayesian Regularization for Acceleration of Levenberg Marquardt based Neural Network Training. *Int J Inte Mult Art Inte* 5: 68. https://doi.org/10.9781/ijimai.2018.04.004
36. Garoosiha H, Ahmadi J, Bayat H (2019) The assessment of Levenberg–Marquardt and Bayesian Framework training algorithm for prediction of concrete shrinkage by the artificial neural network. *Cogent Eng* 6: 1609179 https://doi.org/10.1080/23311916.2019.1609179
37. Abiodun O, Jantan A, Omolara A, et al. (2018) State of the art in artificial neural network applications: A survey. Heliyon 4: E00938. https://doi.org/10.1016/j.heliyon.2018.e00938

AIMS Press